Background on Statistical Modeling of Lava Flows[1]

Chuck and Laura Connor, Jacob Richardson, Lis Gallant

September 6, 2018

[1] Prepared for the COV workshop on Volcanic Hazards for Critical Facilites

What is a lava flow?

Lavas are effusive flows of magma at the surface. That is, they occur when magma reaches the surface of the Earth or other planetary body as a bubbly flow, without experiencing fragmentation. On Earth, lavas are almost always silicates in composition, but lava flows of sulfur and carbon-rich magmas also occur. On land, lava flows are massive volcanic phenomena that inundate areas at high temperature (800 °C – 1250 °C), destroying structures, even whole towns, by entombing them within meters of rock [Branca et al., 2017].

Lava flows are only distinguished from lava domes, such as Chaos Crags at Lassen volcano, by their elongate nature. The main factors that govern lava flow length are the discharge rate of lava at its vent, the physical characteristics of lava, such as viscosity, the topography on to which the lava flows, and the environment of the flow (whether it erupts under water, ice, or in some other atmosphere).

The rate of advance of lava flows is generally slow, measured in meters per hour or per day. A few eruptions, like the 2002 eruption of Nyiragongo volcano (Democratic Republic of the Congo), produce very low viscosity melts, which can travel downslope at meters per second and are too fast to outrun. Nevertheless, the vast majority of lava flows do damage by burying the landscape with a slow but unstoppable advance. Lava flows transform the landscape, and generally land buried by a lava flow is permanently abandoned to all uses, except tourism. Lava flow hazards include rock-fall from the sides of the lava flow even long after is stops advancing, emission of volcanic gases, which can have a substantial downwind impact over a long period of time, and wild-fires.

Humanity has yet to experience the full impact of very voluminous lava flow eruptions. The geological and historical records suggest that impacts of degassing from voluminous lava flows ($> 10\,km^3$) may be continental or global in scale [Rampino, 2002, Self et al., 2005]. We know of no lava flow model that couples hazards, such as gas emission, or wild-fire potential, so there is ample room for progress!

Figure 1: A thin, relatively low viscosity lava flow, the Pahoa flow from Kilauea volcano (HI; photo from USGS). These pāhoehoe lava flows are typically 1–10 m thick, but can have startlingly complex behaviors.

Figure 2: An ʻa ʻā lava flow advancing slowly at Mt Etna. These lava flows have intermediate viscosity and are typically 5–30 m thick. Rubble forms because the surface of the lava flow cools and crystallizes, forming a crust, while the interior remains molten. This crust breaks up as the flow continues to advance.

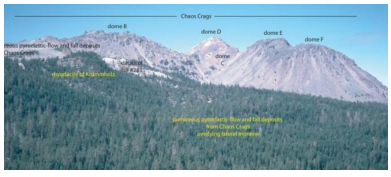

Figure 3: The Chaos Crags, Lassen volcano, are an example of lava domes (USGS photo). These blocky lava flows and domes are often 10 – 300 m thick. The large blocks comprising these domes are indicative of high eruption viscosities.

Problems forecasting lava flow hazards

LAVA FLOW MODELS ARE USED TO FORECAST AREAS OF INUNDATION, given an event of a particular magnitude and location. A lava flow model simulates the effusion of lava from a vent, perhaps calibrated by field measurements of thicknesses and volumes of previously erupted lava flows within an area encompassing the site of interest. The simulated lava flows follow the topography, represented by a digital elevation model (DEM).

The location of the volcanic vent from which lava will issue is often unknown in advance of a volcanic eruption. The eruption may occur from a previously active volcanic vent, or the eruption may result in the formation of an entirely new vent. Vent location is of primary importance in assessing the potential for a given area to be inundated by lava. In long term hazard assessments, this uncertainty in vent location is treated using statistical models of vent spatial density [Connor et al., 2012, ElDifrawy et al., 2013].

The quality of the DEM is a major concern and the DEM may change rapidly during the onset of eruptive activity, due to cone-building, deformation and related factors. For example, the silicic lava flow erupted during the Cordon-Caulle (Chile) eruption appears to have been deflected by the topographic deformation associated with intrusion of a shallow laccolith [Castro et al., 2016].

There is great uncertainty about the volume and effusion rate of potential lava flows. lengths of channelized lava flow are proportional to effusion rate [Kilburn, 2000]. Effusion rates are still rarely observed directly. Change in effusion rate with time has been used to forecast the duration and total eruptive volume once eruptions have initiated [Pedersen et al., 2017, Bonny and Wright, 2017].

In order to model the physics of lava motion, one must consider diverse mechanisms for heat transfer (radiation, conduction, convection), formation and destruction of crust, time dependent and spatially variable viscosity due to cooling, crystallization and bubble nucleation. Consequently, physical models of lava flows are simplified. See a recent review of lava flow physics by Tarquini [2017] and the classic paper by Griffiths [2000].

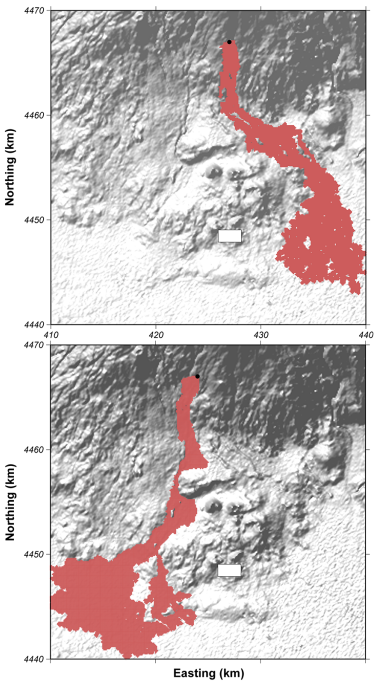

Figure 4: Simulated large-volume flows originating higher up the flanks of Aragats volcano, Armenia. These lava flows are simulated with a volume 0.5 km^3 and a thickness of 3 m, similar to older lava flows in the area.

Numerical Simulation of Lava flows

THE AREA INUNDATED BY LAVA FLOWS DEPENDS ON THE ERUPTION RATE, THE TOTAL VOLUME ERUPTED, AND MAGMA RHEOLOGICAL PROPERTIES, which in turn are a function of composition and

temperature, and the slope of the final topographic surface [Dragoni and Tallarico, 1994, Griffiths, 2000, Costa and Macedonio, 2005]. Previous studies have modeled the physics of lava flows using the Navier-Stokes equations and simplified equations of state [Dragoni, 1989, Del Negro et al., 2005, Miyamoto and Sasaki, 1997]. Other studies have concentrated on characterizing the geometry of lava flows, and studying their development during effusive volcanic eruptions [Walker, 1973, Kilburn and Lopes, 1988, Stasiuk and Jaupart, 1997, Harris and Rowland, 2009]. These morphological studies are mirrored by models that concentrate on the areal extent of lava flows, rather than their flow dynamics. These models generally abstract the rheological properties of lava flows using geometric terms and/or simplified cooling models [Barca et al., 1994, Wadge et al., 1994, Harris and Rowland, 2001, Rowland et al., 2005].

MOLASSES

We created a lava flow model, originally written in PERL [Connor et al., 2012], now in C, to assess the potential of inundation for lava flows. Since the primary information available for lava flows is their thickness, area, length and volume, this model is guided by these measurable parameters and not directly concerned with lava flow effusion rates, their fluid-dynamic properties, or their chemical make-up and composition. The purpose of the model is to determine the conditional probability that flow inundation of a site or area will occur, given an effusive eruption at a particular location, often estimated using the spatial density model.

Input data that are needed to develop a probability model include the spatial distribution of past eruptive vents, the distribution of past lava flows within an area surrounding the site, and measurable lava flow features including thickness, length, volume, and area, for previously erupted lava flows. Thus, the model depends on mappable features found in the site area. Given these input data, Monte Carlo simulations generate many possible vent locations and many possible lava flows, from which the conditional probability of site inundation by lava flow, given the opening of a new vent, is estimated.

A total volume of lava to be erupted is set at the start of each model run. The model assumes that each DEM cell inundated by lava retains or accumulates a residual amount of lava. The residual thickness that is retained by cell must be reached before that cell will pass any lava to adjacent cells. This residual corresponds to the modal thickness of the lava flow. Lava may accumulate in any cell to amounts greater than this residual value if the topography allows pooling of lava. Some algorithms used to distribute lava use a resid-

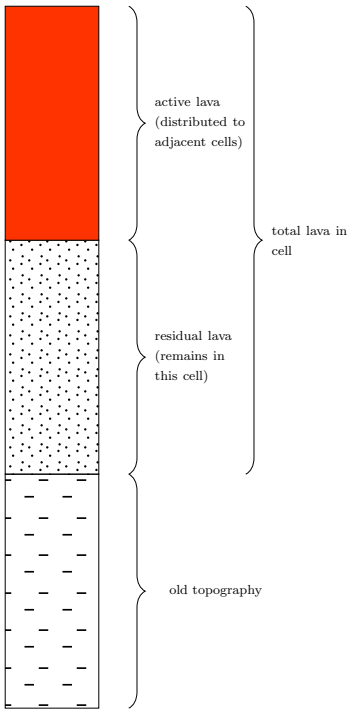

Figure 5: In MOLASSES, parent cells are DEM grid cells that have lava available to give away to near-neighbors. Some lava accumulates and freezes in the parent cell, forming the residual. The active lava is available to give to other cells. Note that the model does not imply any specific geometry or physical state (e.g., the active lava may be beneath a crust of residual lava; active lava may be completely molten, or include mobile blocks within the flow).

ual that varies as a function of slope of the pre-existing topography. As flow thickness varies between lava flows, the residual value chosen for the flow model also varies from simulation to simulation. Here, our term *residual* corresponds to the term *adherence*, used in codes developed by Wadge et al. [1994] and Barca et al. [1994]. In our case, residual lava does not depend on temperature or viscosity, but rather, is used to maintain a modal lava flow thickness. Based on the thicknesses of lava flows measured within the site area, a residual value is randomly chosen to represent the modal thickness of each simulated flow. The measured thicknesses of various lava flows are then fit to a statistical distribution. The model randomly selects a residual value from this best-fit distribution.

Lava flow simulation requires a DEM of the region of interest. One source of easily available topographic data is the SRTM database. The 30-meter or 90-meter grid spacing of SRTM data limits the resolution of the lava flow. Topographic details smaller than 90 m can influence flow path but these cannot be accounted for using a 90-m DEM. More detailed DEM's, such as the 30-m DEM for Mt. Lassen, can provide enhanced flow detail, but a decrease in DEM grid spacing increases the total number of grid cells, thus increasing computation time as the flow has to pass through an increasing number of grid cells [Kubanek et al., 2015]. A balance needs to be maintained between capturing important flow detail over the topography and limiting the overall time required to calculate the full-extent of the flow.

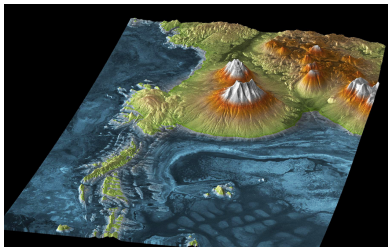

Figure 6: An oblique view of a TanDEM-X DEM for the Uyuni Salar volcanic region, Bolivia. From the Airbus web page.

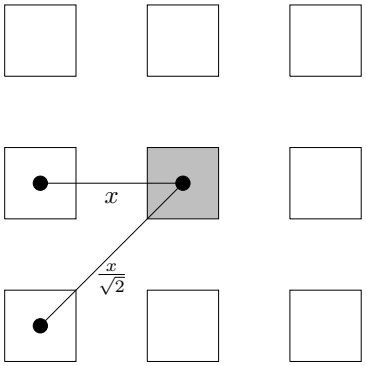

Figure 7: An active cell (gray) distributes lava to its neighboring cells. The Moore neighborhood is used with cells positioned orthogonal to the grid receiving proportionally more lava than those neighboring cells located on diagonals, based on the weighted distance between cell centers.

Structure of MOLASSES

An algorithm is used to distribute the lava from a source cell to each of its adjacent cells once the residual of lava has accumulated. This algorithm passes lava among adjacent cells defined by the DEM. Four orthogonal cells are defined as those cells directly north, south, east and west of a parent cell, which is the source of lava (assuming the DEM is a grid oriented parallel to the Cardinal directions). Four diagonal cells are oriented on the diagonal compared to the parent cell and the orientation of the grid. For ease of calculation, volumes are changed to thicknesses because the area of cells on DEMs is everywhere the same.

Cells that receive lava are added to a list of *active* cells to track relevant properties regarding cell state, including: location within the DEM, current lava thickness, and initial elevation. Active cells have at least one *parent* cell, from which they receive lava, and may have *neighbor* cells which receive their excess lava. A cell becomes a neighbor only if its effective elevation (*i.e.* lava thickness + original elevation) is less than its parent's effective elevation. If an active cell

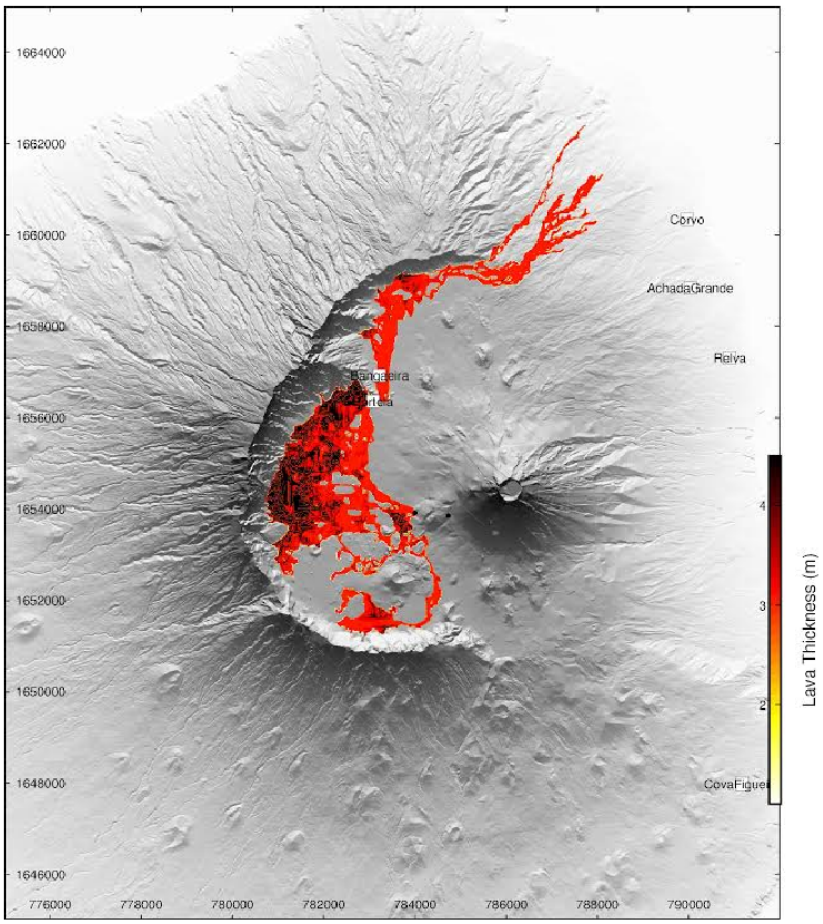

Figure 8: Our lava flow simulation made in December 2014 with an older version of the code to assess the potential for lava flows to reach the town of Corvo (Cabo Verde) and adjacent areas, if the lava flow continued to erupt. Total lava flow volume for this simulation was 50,000,000 m^3.

has neighbors, then its excess lava is distributed proportionally to each neighbor.

MOLASSES has a cellular automata design. The code is implemented in a modular fashion, with the goal of making it easy to test alternative ways to distribute lava from parent to neighbor grid cells. These different rules affect the form of the lava flow – its length, width, and thickness.

Overall, MOLASSES uses the following structure to distribute lava:

```
Until counter reaches the most recently activated cell in activeList:
      IF a cell on the active list has enough lava to spread:
          Identify cells in local neighborhood which can receive lava
          IF there are cells:
             Define volume to advect away from center cell
             Calculate Cell-Cell elevation reliefs and sum them
             FOR each neighbor:
               Determine Effective center cell - neighbor Cell relief
               If neighbor cell is not in activeList, append with ACTIVATE
               Determine volume to add to neighbor cell
               Add thickness of lava to neighbor cell
               Reduce lava volume in center cell by total volume distributed
 Increment counter and test against number of cells in activeList

RETURN:
Updated number of active cells
```

So far we have implemented four different algorithms for determining the volume (thickness of lava in each equal area DEM grid cell) to be distributed from the parent cell and how this volume is distributed among the neighbor cells. These different algorithms affect the flow characteristics.

Equal Spreading Distribution

In equal spreading, the same volume of lava is distributed from parent cells to neighbor cells, regardless of the topographic differences between parent and neighbor cells, until the effective elevation among the parent and neighbor cells is equal or the lava flow stops (the entire volume is erupted).

$$X_p = N_o T_o + N_d T_d \tag{1}$$

where X_p is the excess lava to be distributed from the parent cell to the neighboring cells, N_o is the number of neighbors that will receive

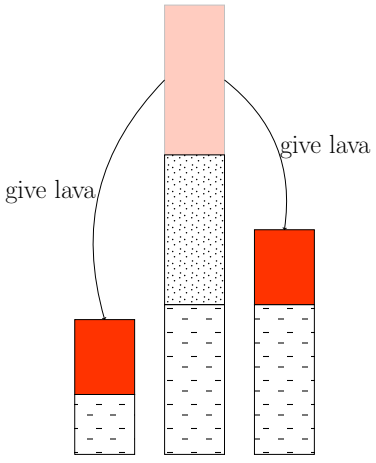

Figure 9: The equal spreading distribution algorithm The two neighbors get equal fraction of the lava distributed from the parent cell, regardless of the elevation differences between them.

lava in the orthogonal direction (the orthogonal neighbors in the Moore neighborhood), N_d is the number of diagonal neighbors in the Moore neighborhood, T_o is the fraction of lava given to each orthogonal neighbor and T_d is the fraction of lava given to each diagonal neighbor.

$$T_d = \frac{T_o}{\sqrt{2}} \tag{2}$$

$$T_o = \frac{X_p}{\left[N_o + \frac{N_d}{\sqrt{2}}\right]} \tag{3}$$

So the amount of lava distributed to each neighbor is determined by the number of orthogonal and diagonal neighbors. The number of active neighbors a parent cell is variable, primarily controlled by local topographic variation as represented by the DEM. If the lava distributed to a cell causes the residual lava thickness to be exceeded, then that lava must be redistributed (this neighbor becomes a parent in the next iteration).

Lava flows simulated in using the equal spreading distribution algorithm tend to spread laterally on across the slope. This algorithm appears to mimic the behavior of thicker, more viscous lava flows with higher yield strength. The force moving lava radially from the vent is significant compared to the gravitational force acting in the downslope direction.

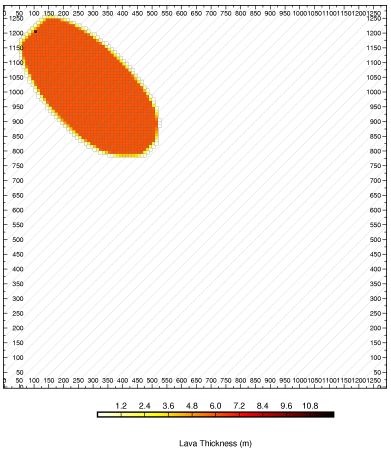

Figure 10: A test of the equal-spreading distribution algorithm with constant residual. The flow, erupted on to a 45° slope from the point indicated by the red circle, tends to spread in the cross-slope direction. The interior of the flow has a uniform thickness corresponding to the user specified residual.

Spreading Proportional to Slope Distribution

One can also weight the fraction of the excess lava, X_p, distributed to each neighbor cell, T_o and T_d by the elevation difference between each parent and each neighbor cell. In this model more lava is given to neighbor cell that is downslope of the parent compared to a neighbor that is across-slope from the parent.

Using spreading-proportional-to-slope, lava flows become more elongate on a given slope compared to stubby flows produced by the equal distribute algorithm. This may be more appropriate for relatively low viscosity lavas.

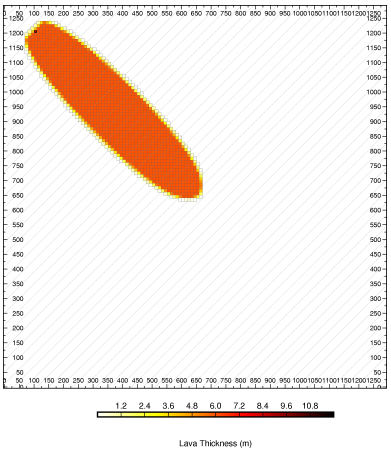

Figure 11: A test of the spreading-proportional-to-slope distribution algorithm with constant residual. The flow, erupted on to a 45° slope from the point indicated by the red circle, tends to become more elongate downslope compared to the equal spreading distribution algorithm. The interior of the flow has a uniform thickness corresponding to the user specified residual. All inputs (flow volume, thickness, volume erupted per iteration, the DEM) are the same as in Figure 10, only the distribution algorithm is changed.

Slope Dependent Residual

Some lava flows thin on steep slopes. The amount of thinning that occurs is likely related to the effusion rate and time-dependent viscosity relative to the slope. Griffiths [2000] showed that a critical thickness exists for viscoplastic flows, below which the flow will not move. The critical depth is:

$$h_s = \frac{\sigma_o}{\rho g \sin \beta} \tag{4}$$

where σ_o is the critical yield strength (e.g., 1×10^5 Pa), ρ is lava density (e.g., 2200 kg m^{-3}), g is gravitational acceleration (e.g., 10 m s^{-2}), and β is the slope angle. Lavas have a wide range of σ_o, so may have a range of thicknesses on a simple slope.

Both the proportional-to-slope spreading and equal-spreading algorithms can be modified by making the residual itself proportional to slope. This is implemented by making the residual of a new active cell proportional to the slope between it and its parent cell.

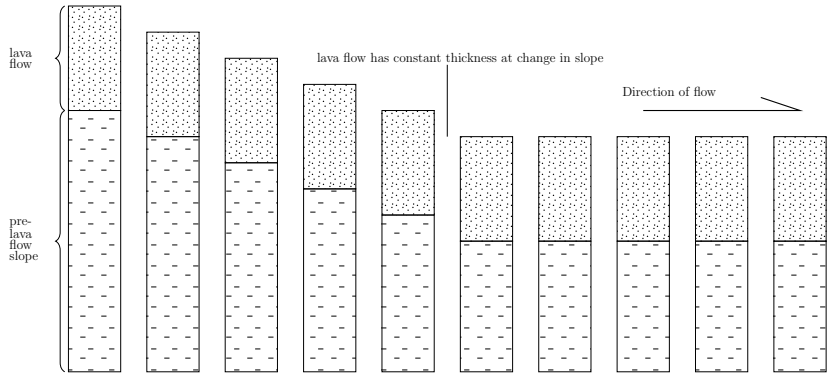

Figure 12: A lava flow with a constant residual, independent of the slope it erupts on to.

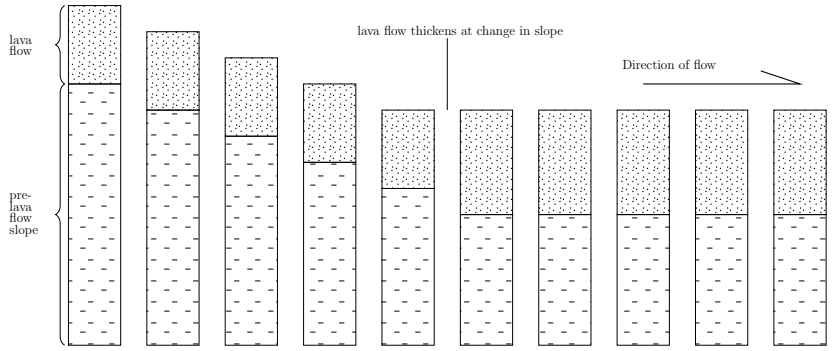

Figure 13: A lava flow with residual that depends on the slope of the pre-existing terrain.

This yields a total of four distribution algorithms in MOLASSES that we have implemented so far:

- Equal spreading with constant residual (Figure 10)
- Spreading proportional to slope with constant residual (Figure 11)
- Equal spreading with residual that depends on slope between the parent cell and the neighbor cell (Figure 18)
- Spreading proportional to slope with residual that depends on the slope between the parent and neighbor cell (Figure 19)

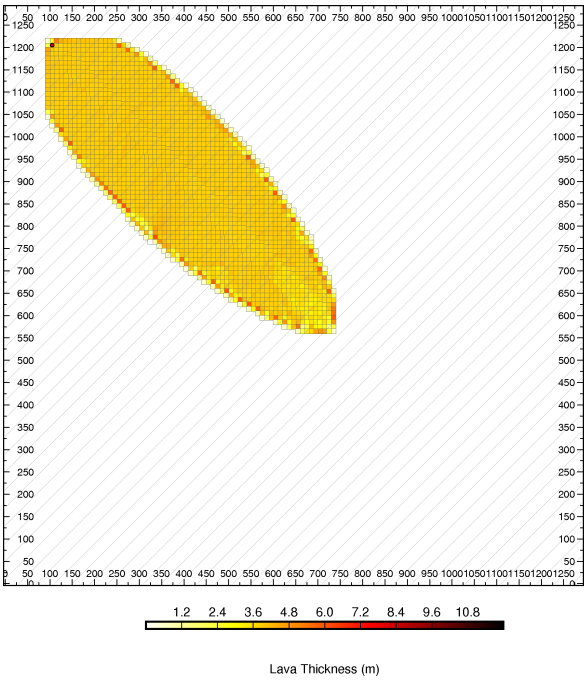

Figure 14: A test of the modified equal spreading distribution algorithm with residual depending on slope angle. The flow, erupted on to a 45° slope from the point indicated by the red circle, tends to become more elongate downslope compared to the equal spreading distribution algorithm with constant residual. Note that the flow surface develops topography, even on a planar inclined DEM. The flow is thickest at the flow margins (levees) and thins slightly along its centerline. All inputs (flow volume, thickness, volume erupted per iteration, the DEM) are the same as in Figure 10, only the distribution algorithm is changed.

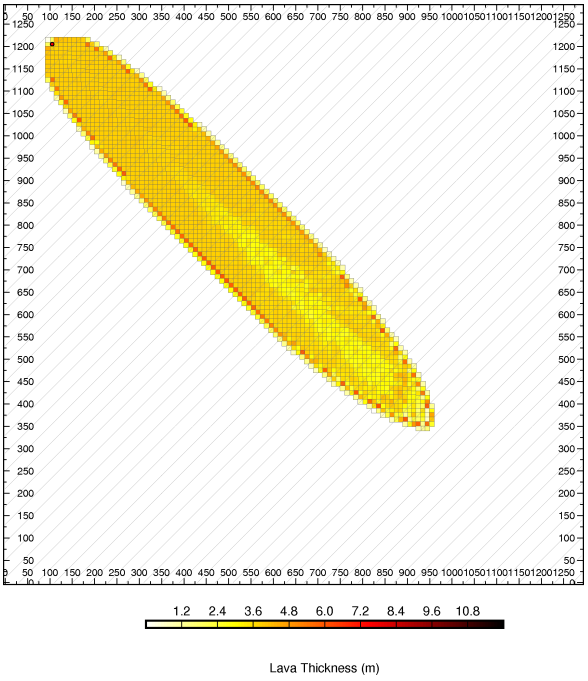

Figure 15: A test of the modified proportional to slope distribution algorithm with residual depending on slope angle. The flow, erupted on to a 45° slope from the point indicated by the red circle, tends to become more elongate downslope compared to other spreading algorithms. Flow surface topography is also the most highly developed in this model, with levees and a distinctive channel forming. Inputs (flow volume, thickness, volume erupted per iteration, the DEM) are the same as in Figure 10, only the distribution algorithm is changed.

It is worth comparing all four test maps to observe the importance of the choice of algorithm for the shape of the lava flow. An interesting feature of the slope-dependent residual output is that lava flow levees and channels develop in the flows. This complexity surprised us, given the simplicity of the distribute algorithms. We suggest that further modifications of these distribute algorithms will produce useful results.

Application to a complicated DEM: Mt. Lassen

The test examples give a simplified view. What affect does distribute algorithm choice have on the flow pattern on a more complicated DEM? Compare the following maps made with the same input parameters for a rather complicated lava flow in the Mt. Lassen area.

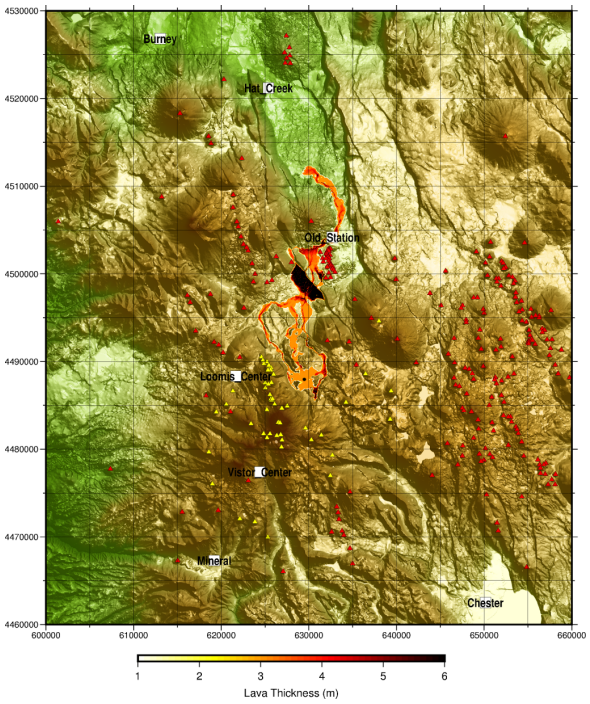

Figure 16: The equal-spreading distribution algorithm with constant residual applied to a lava flow simulated on the East side of Mt. Lassen.

The lava flow is sourced on a volcano located East of the Loomis Center and East of Chaos Crags. The lava flow forms several channels, and pools at a fault scarp between the Loomis Center and the Old Station.

Compare the lava flow depth near the vent (black circle) and the area inundated with the following maps that use different distribute algorithms.

Probability and MOLASSES

Probabilistic hazard assessment is one use of MOLASSES. Lis Gallant used MOLASSES to model the likelihood of lava flow inundation of the Idaho National Lab (ID). She set up the model by modeling the spatial density of volcanic vents on the Eastern Snake River Plain using an elliptical kernel. She explored the sensitivity of the model to varying definitions of volcanic events (sometimes grouping more

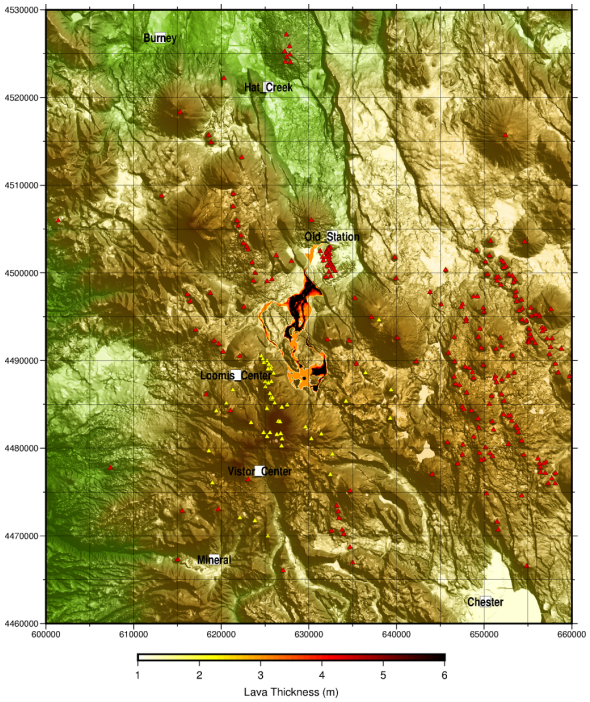

Figure 17: The spreading-proportional-to-slope distribution algorithm with constant residual. All inputs (flow volume, thickness, volume erupted per iteration, the DEM) are the same as in Figure 16, only the distribution algorithm is changed.

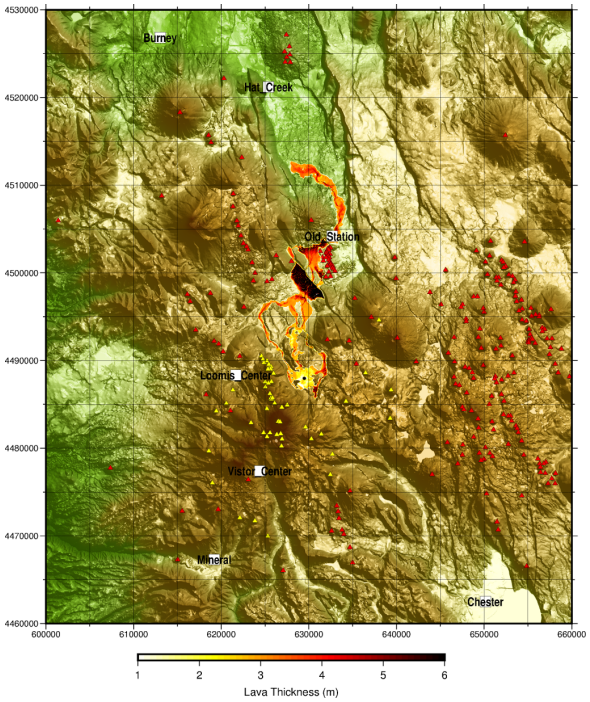

Figure 18: The equal spreading distribution algorithm with slope dependent residual. All inputs (flow volume, thickness, volume erupted per iteration, the DEM) are the same as in Figure 16, only the distribution algorithm is changed.

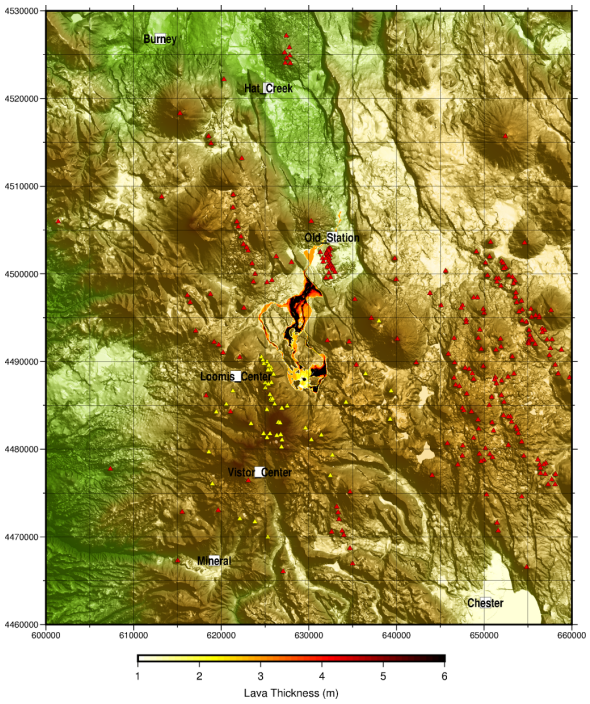

Figure 19: The spreading-proportional-to-slope distribution algorithm with slope dependent residual. All inputs (flow volume, thickness, volume erupted per iteration, the DEM) are the same as in Figure 16, only the distribution algorithm is changed.

than one vent into a single event). She then used the volume and thickness estimates of past lava flows to forecast future flows.

She simulated a total of 10,000 lava flows using MOLASSES. A total of 2,545 breached the boundaries of INL and 1,827 initiated within its boundaries. In contrast, the city of Idaho Falls was inundated by 10 simulated lava flows. Pocatello was not inundated in any simulation. Additionally, 10,000 flows were simulated for eruptions initiating from a list of events; of these simulated lava flows 3,374 partially inundated INL and 2,585 events erupted within the laboratory's boundaries. In these simulations, Idaho Falls was inundated 36 times. As in the previous simulation, Pocatello was not inundated by lava flows. The probability of partial inundation of the INL is approximately 25–34% given a future eruption. This range primarily represents uncertainty about the number of eruptions represented by mapped volcanic vents, as the INL represents only approximately 8% of the total area of the ESRP. Model results suggest this relatively high conditional probability arises due to the position of the INL in an area of spatially dense volcanic activity and because of the low topography of the site, which tends to focus lava flows from vents outside the INL boundaries.

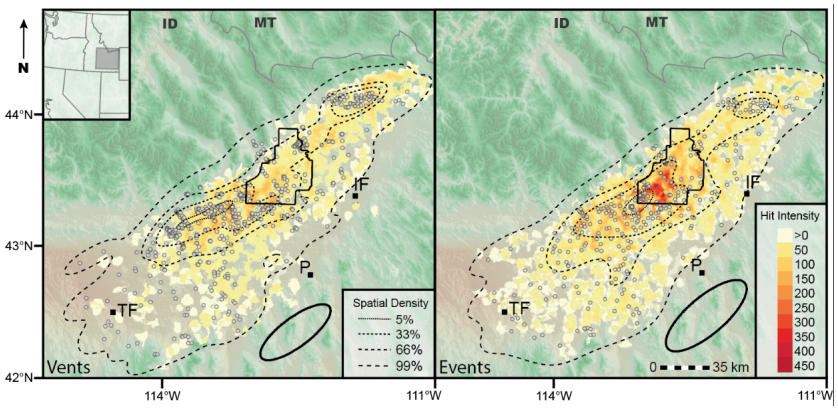

Figure 20: Simulation outputs for a probabilistic hazard model of lava inundation for the Idaho National Lab (INL), made using MOLASSES. The solid line shows the outline of INL area. TF= Twin Falls, P= Pocatello, IF= Idaho Falls. Left: Map of 10,000 lava flows erupted from vents. 2,545 flows inundate INL. The scale on the right indicates hit intensity. The white dots indicate modeled vent locations. The ellipse represents the vent spatial density kernel. Right: Map of 10,000 simulated lava flows erupted from events. 3,374 flows inundate INL. The white dots indicate modeled event locations. The ellipse represents the event spatial density kernel

References

D. Barca, G. M. Crisci, S. Di Gregorio, and F. Nicoletta. Cellular automata for simulating lava flows: A method and examples of the Etnean eruptions. *Transport Theory and Statistical Physics*, 23: 195–232, 1994.

Estelle Bonny and Robert Wright. Predicting the end of lava flow-forming eruptions from space. *Bulletin of Volcanology*, 79(7):52, 2017.

Stefano Branca, Emanuela De Beni, David Chester, Angus Duncan, and Alessandra Lotteri. The 1928 eruption of Mount Etna (Italy): Reconstructing lava flow evolution and the destruction and recovery of the town of Mascali. *Journal of Volcanology and Geothermal Research*, 335:54–70, 2017.

Jonathan M Castro, Benoit Cordonnier, C Ian Schipper, Hugh Tuffen, Tobias S Baumann, and Yves Feisel. Rapid laccolith intrusion driven by explosive volcanic eruption. *Nature Communications*, 7: 13585, 2016.

Laura J Connor, Charles B Connor, Khachatur Meliksetian, and Ivan Savov. Probabilistic approach to modeling lava flow inundation: a lava flow hazard assessment for a nuclear facility in Armenia. *Journal of Applied Volcanology*, 1(1):3, 2012.

A. Costa and G. Macedonio. Computational modeling of lava flows: A review. *Geological Society of America Special Papers 396*, pages 209–218, 2005. DOI: 10.1130/0-8137-2396-5.209.

C. Del Negro, L. Fortuna, and A. Vicari. Modelling lava flows by cellular nonlinear networks (CNN): preliminary results. *Nonlinear Processes in Geophysics*, 12:505–513, 2005.

M. Dragoni. A dynamical model of lava flows cooling by radiation. *Bulletin of Volcanology*, 51:88–95, 1989.

M. Dragoni and A. Tallarico. The effect of crystallization on the rheology and dynamics of lava flows. *Journal of Volcanology and Geothermal Research*, 59:241–252, 1994.

MA ElDifrawy, MG Runge, MR Moufti, SJ Cronin, and M Bebbington. A first hazard analysis of the Quaternary Harrat Al-Madinah volcanic field, Saudi Arabia. *Journal of Volcanology and Geothermal Research*, 267:39–46, 2013.

R. W. Griffiths. The dynamics of lava flows. *Annual Review of Fluid Mechanics*, 32:477–518, 2000.

A. J. L. Harris and S. K. Rowland. FLOWGO: a kinematic thermo-rheological model for lava flowing in a channel. *Bulletin of Volcanology*, 63:20–44, 2001.

A. J. L. Harris and S. K. Rowland. Controls on lava flow length. In T. Thordarson, S. Self, G. Larsen, S. K. Rowland, and A. Höskuldsson, editors, *Studies in Volcanology, The Legacy of George Walker*, Special Publications for IAVCEI No. 2, pages 33–51. The Geological Society, London, 2009.

C. J. R. Kilburn and R. M. C. Lopes. The growth of aa lava fields on Mt. Etna, Sicily. *Journal of Geophysical Research*, 93:14759–14722, 1988.

Christopher RJ Kilburn. Lava flows and flow fields. *Encyclopedia of Volcanoes*, pages 291–305, 2000.

Julia Kubanek, Jacob A Richardson, Sylvain J Charbonnier, and Laura J Connor. Lava flow mapping and volume calculations for the 2012–2013 Tolbachik, Kamchatka, fissure eruption using bistatic TanDEM-X InSAR. *Bulletin of Volcanology*, 77(12):106, 2015.

N Miyamoto and S. Sasaki. Simulating lava flows by an improved cellular automata method. *Computers and Geosciences*, 23:283–292, 1997.

GBM Pedersen, A Höskuldsson, Tobias Dürig, Thorvaldur Thordarson, Ingibjorg Jonsdottir, Morten S Riishuus, BV Óskarsson, S Dumont, Eyjólfur Magnússon, Magnus Tumi Gudmundsson, et al. Lava field evolution and emplacement dynamics of the 2014–2015 basaltic fissure eruption at Holuhraun, Iceland. *Journal of Volcanology and Geothermal Research*, 340:155–169, 2017.

Michael R Rampino. Supereruptions as a threat to civilizations on earth-like planets. *Icarus*, 156(2):562–569, 2002.

S. K. Rowland, H. Gabriel, and A. J. L. Harris. Lengths and hazards of channel-fed lava flows on Mauna Loa (Hawaii), determined from thermal and downslope modeling with FLOWGO. *Bulletin of Volcanology*, 67:634–647, 2005.

Stephen Self, Thorvaldur Thordarson, and Mike Widdowson. Gas fluxes from flood basalt eruptions. *Elements*, 1(5):283–287, 2005.

Mark V. Stasiuk and Claude Jaupart. Lava flow shapes and dimensions as reflections of magma system conditions. *Journal of Volcanology and Geothermal Research*, 78(1-2):31–50, 1997. DOI: 10.1016/S0377-0273(97)00002-4.

Simone Tarquini. A review of mass and energy flow through a lava flow system: insights provided from a non-equilibrium perspective. *Bulletin of Volcanology*, 79(8):64, 2017.

G. Wadge, P. A. V. Young, and I. J. McKendrick. Mapping lava flow hazards using computer simulation. *Journal of Geophysical Research*, 99:489–504, 1994.

G. P. L. Walker. Lengths of lava flows. *Philosophical Transactions of the Royal Society, London*, 274:107–118, 1973.